Composites Science and Technology 72 (2012) 1479–1486

Contents lists available at SciVerse ScienceDirect

Composites Science and Technology

journal homepage: www.elsevier.com/locate/compscitech

Hierarchical composites reinforced with robust short sisal fibre preforms utilising bacterial cellulose as binder

Koon-Yang Lee [a], Kingsley K.C. Ho [a,1], Kerstin Schlufter [b], Alexander Bismarck [a,*]

[a] Polymer and Composite Engineering (PaCE) Group, Department of Chemical Engineering, Imperial College London, South Kensington Campus, London SW7 2AZ, UK
[b] fzmb GmbH Research Centre of Medical Technology and Biotechnology, D-99947 Bad Langensalza, Germany

ARTICLE INFO

Article history:
Received 23 January 2012
Received in revised form 8 June 2012
Accepted 16 June 2012
Available online 2 July 2012

Keywords:
A. Short-fibre composites
A. Polymer–matrix composites (PMCs)
B. Fibre/matrix bond
B. Interface
Bacterial cellulose

ABSTRACT

A novel robust non-woven sisal fibre preform was manufactured using a papermaking process utilising nanosized bacterial cellulose (BC) as binder for the sisal fibres. It was found that BC provides significant mechanical strength to the sisal fibre preforms. This can be attributed to the high stiffness and strength of the BC network. Truly green non-woven fibre preform reinforced hierarchical composites were prepared by infusing the fibre preforms with acrylated epoxidised soybean oil (AESO) using vacuum assisted resin infusion, followed by thermal curing. Both the tensile and flexural properties of the hierarchical composites showed significant improvements over polyAESO and neat sisal fibre preform reinforced polyAESO. These results were corroborated by the thermo-mechanical behaviour of the (hierarchical) composites, which showed an increased storage modulus and enhanced fibre–matrix stress transfer. Micromechanical modelling was also performed on the (hierarchical) composites. By using BC as binder for short sisal fibres, added benefits such as the high Young's modulus of BC, enhanced fibre–fibre and fibre–matrix stress transfer can be utilised in the resulting hierarchical composites.

1. Introduction

Significant research effort has been poured into the manufacturing of sustainable materials due to public's growing demand for more environmentally friendly products, depletion of petroleum resources, the ever-growing problem of landfill of waste and heavy environmental legalisation [1]. Natural fibres have gained significant attention as potential replacement for glass fibres to produce greener composites. The advantages of natural fibres as reinforcement for polymers include low density, wide availability and biodegradability [2]. In addition to this, natural fibres possess decent mechanical properties [3]. However, natural fibres suffer from drawbacks such as poor compatibility with hydrophobic polymer matrices and its inherent variability in both fibre properties and dimensions, even within the same cultivation [4]. There is very little that can be done in terms of the variability of their properties and dimensions. However, significant research effort has been poured into modifying the fibres to enhance the fibre–matrix interface [5].

One method of modifying the fibre–matrix interface is to attach bacterial cellulose (BC) onto the surface of natural fibres [6–8]. BC is highly crystalline nano-sized cellulose (24–86 nm in diameter and several micrometres in length [9]) without impurities such as hemicellulose or lignin and possesses a degree of crystallinity of up to 90% [10]. The Young's modulus of a single BC nanofibre was reported to be 114 GPa [11], with theoretical cellulose crystal modulus being as high as 160 GPa [12]. In addition to this, BC also possesses a linear thermal coefficient of expansion (LTCE) of only $0.1 \times 10^{-6}\,K^{-1}$ [13]. By culturing cellulose-producing bacteria, such as from the *Acetobacter* species [9], in the presence of natural fibres, BC is preferentially deposited *in situ* onto the surface of natural fibres. The introduction of BC onto natural fibres provides a new means of controlling the interaction between natural fibres and polymer matrices. Coating of natural fibres with BC does not only facilitate good distribution of BC within the matrix, it also results in an improved interfacial adhesion between the fibres and the matrix [6–8]. This enhances the interaction between natural fibres and a polymer matrix. In addition to culturing cellulose-producing bacteria in the presence of natural fibres to coat the fibres, a method based on slurry dipping was developed recently to coat the surface of sisal fibres with BC [14]. This method utilises the water absorbing capability of natural fibres to absorb the water in BC dispersion, drawing along the nanocellulose in the dispersion onto the surface of the fibres.

In this work, we extend our slurry dipping method to create non-woven sisal fibre preforms for thermosetting matrices. Natural fibres can be stitched or stapled together using polymer fibres

* Corresponding author. Tel.: +44 (0)20 7594 5578; fax: +44 (0)20 7594 5638.
E-mail address: a.bismarck@imperial.ac.uk (A. Bismarck).
[1] Present address: Cytec Engineered Materials, Abenbury Way, Wrexham Industrial Estate, Wrexham LL13 9UZ, UK.

0266-3538
http://dx.doi.org/10.1016/j.compscitech.2012.06.014

to produce non-woven fibre preforms [15–18]. In addition to this, fibre preforms can also be produced by spraying a polymer solution onto the fibre mat followed by heat pressing to consolidate the polymer to bind the fibres together [19]. Natural fibres can be blended with a thermoplastic polymer and melt pressed to create the fibre preform [20]. To process them into composites, these polymeric binder based natural fibre preforms can then be impregnated with a thermosetting resin to produce natural fibre reinforced composites [19,21,22]. Natural fibre preform reinforced thermoplastic composites can also be produced using film stacking, whereby the fibre preforms are stacked between sheets of polymers in alternative sequence and consolidated [23,24].

Our current study focuses on using BC as binder to produce novel non-woven short sisal fibre preforms, moving away from the conventional polymer binders such as polypropylene, polyesters and epoxies [25]. These natural fibre preforms are infused with epoxidised and acrylated soybean oil (AESO) using vacuum assisted resin infusion (VARI) and thermally cured to produce truly green hierarchical composites. Nature maximises the efficiency of structural materials by organising them hierarchically; the arrangement of the constituents at every level, from the molecular to the macroscopic level [26]. By applying this concept, composites that possess a hierarchical structure should have improved mechanical properties compared to the same composites without this hierarchical structure. Not only does the BC act as binder for the loose fibres, it also simultaneously acts as nanofiller to further enhance the mechanical properties of the hierarchical composites due to its high stiffness and strength. The mechanical properties, thermal degradation and thermo-mechanical behaviour of the hierarchical composites were studied.

2. Materials and methods

AESO (Aldrich, density = 1.04 g cm^{-3}, inhibited with 8500 ppm monomethyl ether hydroquinone) and *tert*-butyl peroxybenzoate, otherwise known as Luperox P (Aldrich, purity $\geqslant$ 98%), were purchased from Sigma–Aldrich and used as the thermosetting monomer and thermal initiator, respectively, in this study. Loose sisal fibres were kindly supplied by Wigglesworth & Co. Ltd. (London, UK). These fibres were grown in East Africa. The harvested crop was left in the field for approximately 3–4 weeks for dew retting in order to allow the combined action of temperature, humidity and bacteria to loosen the fibres. After this retting process, the raw fibres were processed with a rudimentary tool to separate the fibres by hand. The fibres were afterwards washed with water and sun-dried for 1 day. BC was provided by fzmb GmbH as wet pellicle containing 94wt.% water. The synthesis of BC used in this study can be found in literature [27].

2.1. Manufacturing natural fibre preforms

The fibre preforms were manufactured using a papermaking process. Neat sisal fibre preforms were manufactured using 16 g of sisal fibres, cut to approximately 10 mm in length which were soaked in 2 L of de-ionised water overnight. This dispersion of short sisal fibres was then filtered under vacuum onto a 125 mm diameter filter paper (Qualitative filter paper 413, VWR, Lutterworth, UK) using a Büchner funnel. The filter cake was wet pressed twice under a weight of 1 t for 2 min. This wet pressed filter cake was then further dried in an oven at 60 °C overnight under a weight of 10 kg. Short sisal fibres were used instead of long fibres because a more uniform dispersion of fibres in water can be obtained. The fibre preforms produced from short fibres were also more uniform.

In order to use BC as binder for the fibre preforms, 29.6 g of wet BC pellicles (equivalent dry mass of 1.78 g) were cut into small pieces and blended for 1 min using a blender (Breville BL18 glass jug blender, Pulse Home Products Ltd., Oldham, UK) and further homogenised (Polytron PT 10–35 GT, Kinematica, Lucerne, CH) for 2 min in 2 L of de-ionised water to produce a uniform dispersion of nanocellulose. 16 g of sisal fibres, cut to approximately 10 mm in length, were soaked in this nanocellulose dispersion overnight. The fibre preforms were then manufactured following the previously described wet pressing followed by drying method. The weight fraction of BC in these sisal fibre preforms was 10 wt.%. Herein, fibre preforms with neat sisal fibres only and sisal fibres with BC binder are termed sisal fibre preforms and BC-sisal fibre preforms, respectively.

2.2. Manufacturing of natural fibre preform reinforced composites

The composites were manufactured using VARI. A schematic diagram of the VARI setup is shown in Fig. 1. A polyester porous flow medium (15087B, Newbury Engineer Textile, Berkshire, UK) was placed on top of the tooling side (a 460 mm $\times$ 920 mm heating plate equipped with a temperature control unit), which was covered by a layer of polyester film (Melinex PW 122-50-RL, PSG group, London, UK). The natural fibre preforms were sandwiched between two PTFE coated glass release fabrics (FF03PM, Aerovac, West Yorkshire, UK) and placed on top of the polyester porous flow medium. Another polyester porous flow medium was then placed on top of the PTFE glass release fabric. The whole setup was covered with a vacuum bagging film (Capran 519 heat stabilised Nylon 6 blown tubular film, Aerovac, West Yorkshire, UK) and sealed using vacuum sealant tape (SM5127, Aerovac, West Yorkshire, UK).

Prior to the infusion of the resin, the previously prepared fibre preforms were further dried by hot-pressing the preforms at 120 °C and 0.25 t for 15 min. This also reduced the porosity of the fibre preforms, resulting in an increased fibre volume fraction of the final composites. AESO was heated to 80 °C to reduce its viscosity and 5 wt.% of Luperox P relative to the weight of AESO was mixed into the resin. This mixture was then de-gassed at a reduced pressure of 100 kPa at 80 °C for 30 min prior to the infusion step in order to remove all air bubbles entrapped during the mixing of the resin and the initiator. The infusion process starts with an air removal step, whereby vacuum was applied to the system via the tubing on the non-tooling side with the resin inlet tubing sealed off. When the maximum vacuum was achieved (~20 kPa), the VARI setup was left under vacuum for 2 h to ensure that there was no leakage in the setup by constantly monitoring the pressure in the vacuum bag. Once the system was determined to be leakage-free, the liquid resin was fed at the same temperature from the bottom of the polyester porous flow medium on the tooling side through the fibre preforms and exited via the tubing on the non-tooling side. Both the VARI setup and the resin were heated to 80 °C in

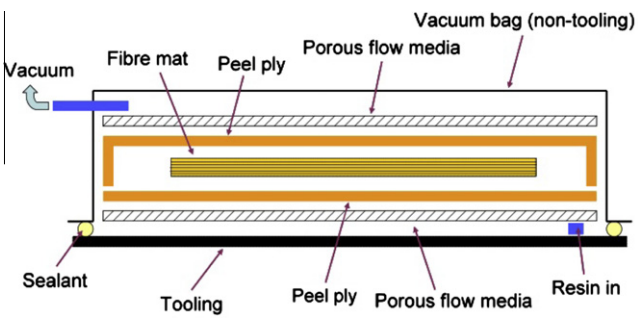

Fig. 1. Schematic diagram of the VARI process.

order to ensure a low enough viscosity of AESO such that it flows readily during the infusion process. The inlet and outlet of the setup were sealed off again once the resin fully penetrated the fibre preforms. The resin was heated to 110 °C for 2 h using a heating rate of 5 °C min^{-1} to cure the resin, followed by a post-curing step at 130 °C for 2 h. The VARI setup was cooled to room temperature prior to the removal of the manufactured composites. The composites reinforced with sisal fibre preforms and BC-sisal fibre preforms are termed sisal-polyAESO and BC-sisal-polyAESO, respectively hereafter. Neat polymerised AESO was produced by pouring the resin into a mould with dimensions of $3 \times 15 \times 20$ mm and polymerised using the same reduced pressure and curing cycle as previously described.

3. Characterisation of the natural fibre preforms and the composites

3.1. Morphology of the natural fibre preforms

Scanning electron microscopy (SEM) was performed using a high-resolution field emission gun scanning electron microscope (LEO Gemini 1525 FEG-SEM, Oberkochen, Germany). It was used to characterise the morphology of the natural fibre preforms using BC as the binder. The accelerating voltage used during SEM was 5 kV. Prior to SEM, the preform was fixed onto SEM stubs using carbon tabs and Cr coated with a sputter coater (K550 sputter coater, Emitech Ltd., Ashford, Kent, UK) for 1 min at 75 mA.

3.2. Tensile properties of the natural fibre preforms

In order to investigate the effect of the BC binder on the mechanical properties of the fibre preforms, tensile tests were conducted on these preforms (without any matrix present) in accordance to BS EN ISO 9073-18:2008. Prior to the test, the fibre preforms were cut into dimensions of $3 \times 15 \times 100$ mm. Woven glass fibre reinforced polyester end tabs with a thickness of 1.6 mm were glued (Araldite 2011, Huntsman Advanced Materials, Cambridge, UK) onto the ends of the test specimens to prevent the clamping jaws of the test machine from damaging the test specimens. The distance between the gauge length was 60 mm. Tensile tests were conducted using an Instron universal material testing equipment (Instron 4505, Instron Corporation, MA, USA) equipped with 1 kN load cell. The specimens were tested using a crosshead speed of 1 mm min^{-1}.

3.3. Density measurements of the fibre preforms and the composites

The density of the fibres, neat polyAESO and its composites was measured using He pycnometry (AccuPyc 1330, Micromeritics Ltd., Dunstable, UK). The samples were weighed prior to placing them in the measuring chamber of the He pycnometer. As the pressure of He rises above the atmospheric value, it was expanded through a value and this expanded volume was measured. Due to the expansion of He, the pressure inside the chamber will decrease to a steady-state value. With the mass of the sample known, the density ρ_m of the sample can then be calculated using the equation:

$$\rho_m = \frac{m_s}{V_c - \frac{V_E}{\frac{P_1}{P_2} - 1}} \quad (1)$$

where m_s is the sample mass, V_c is the volume of the chamber, V_E is the expanded volume of helium, P_1 and P_2 are the chamber's elevated pressure and steady-state pressure, respectively. The apparent density ρ_e of the fibre preforms was calculated from the mass and apparent volume of the preforms. The fibre volume fraction v_f of the composites was calculated based on the densities of the fibre preforms and composites, respectively using the equation:

$$v_f = \frac{\rho_c - \rho_{matrix}}{\rho_f - \rho_{matrix}} \quad (2)$$

where ρ_c, ρ_f and ρ_{matrix} are the densities of the composites, fibre preforms and the poly(AESO), respectively. This v_f value is the total volume fractions of fibres in the composites.

3.4. Mechanical properties of the composites

The composites were tested in tension and flexural (3-point bending) mode using an Instron universal material testing equipment (Instron 4505, Instron Corporation, MA, USA) in accordance to ASTM D 3039-00 and D638-03, respectively. The tensile test specimens possessed dimensions of $3 \times 15 \times 100$ mm, with a gauge length of 30 mm. Prior to the test, woven glass fibre reinforced polyester end tabs with a thickness of 1.6 mm were glued onto the samples using a two-part cold curing epoxy resin (Araldite 2011, Huntsman Advanced Materials, Cambridge, UK). The distance between the end tabs was set to be 60 mm. Strain gauges (FLA-2-11, Techni Measure, Studley, UK) were glued onto the middle portion of the test specimen using cyanoacrylate glue (EVERBUILD Building Products Ltd., Leeds, UK). Tensile tests were conducted using a crosshead speed and load cell of 1 mm min^{-1} and 10 kN, respectively. The flexural test specimens possessed dimensions of $3 \times 15 \times 80$ mm. The span-to-thickness ratio and crosshead speed used in flexural test were 20 and 1 mm min^{-1}, respectively. A total of 5 specimens were tested in each test for each type of samples.

3.5. Thermo-mechanical behaviour of the composites

The viscoelastic behaviour of polyAESO and the composites was characterised using dynamic mechanical thermal analysis (DMTA) (Tritec 2000, Triton Technology Ltd., Keyworth, UK). DMTA was conducted in single beam cantilever bending mode with a gauge length of 10 mm. The sample had a width and an average thickness of 4 mm and 3 mm, respectively. The storage modulus, loss modulus and energy dissipation factor (tan δ) were measured from −95 °C to 180 °C at a heating rate of 5 °C min^{-1} and a frequency of 1 Hz.

3.6. Thermal stability of the composites: thermal gravimetric analysis (TGA)

The thermal degradation behaviour of sisal fibres, BC, neat polyAESO and its composites was characterised using TGA (TGA Q500, TA Instruments, UK). Samples of 35 mg were heated from room temperature to 600 °C in N_2 at a heating rate and N_2 flowrate of 5 °C min^{-1} and 60 mL min^{-1}, respectively.

4. Results and discussion

4.1. Tensile properties of the natural fibre preforms

The mechanical performance of the fibre preforms under tension is shown in Table 1, along with the porosity of the fibre preforms. The tensile strength tabulated in this table is defined as the maximum load required to break the sample per unit width of the specimen (15 mm) as the cross-sectional area of the fibre mat is not well defined. With BC as the binder, a tensile strength of 13.1 kN m^{-1} was achieved. However, the tensile strength of the neat sisal fibre preforms was not measureable. This is due to the fact that these sisal fibres are loose and held together only by

Table 1
Properties of natural fibre preforms: σ_w, ρ_m, ρ_e and P denote the tensile strength, absolute density, apparent density and porosity of the fibre preform, respectively.

Fibre preforms	σ_w (kN m^{-1})	ρ_m (g cm^{-3})	ρ_e (g cm^{-3})	P (%)
Sisal	Not measureable	1.298 ± 0.004	0.350 ± 0.018	73 ± 5
BC-sisal	13.1 ± 2.1	1.318 ± 0.004	0.514 ± 0.015	61 ± 3

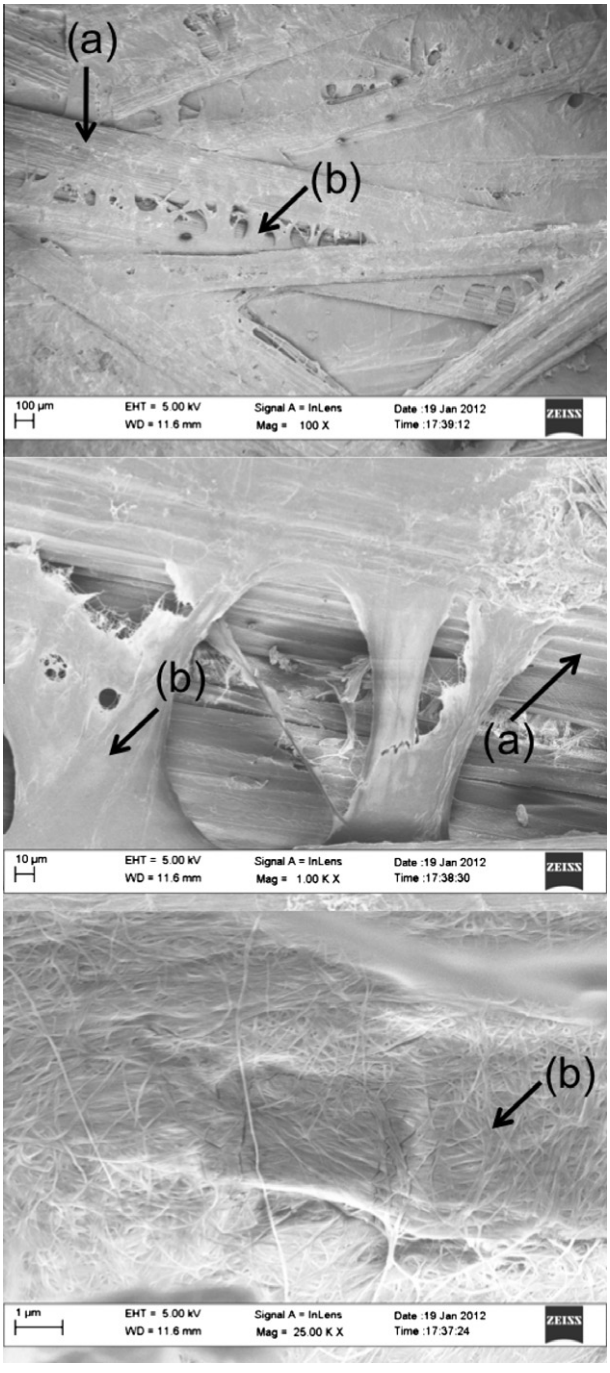

Fig. 2. Scanning electron micrographs of natural fibre preform using BC as binder at various magnifications. Top: 100×, middle: 1000 × and bottom: 25000×, respectively. (a) and (b) denote the sisal fibre and BC nanofibrils, respectively.

friction between the fibres even after the wet pressing step to consolidate them into fibre preforms. The improved mechanical performance of BC-sisal fibre preforms can be attributed to the use of BC as the binder, which also promotes fibre–fibre stress transfer. The nano-sized BC holds the otherwise loose sisal fibres together (see Fig. 2) due to hornification (irreversible hydrogen bonding between the nanocellulose) [28]. It was found that BC sheets have very high tensile strength of approximately 300 MPa (estimated to be approximately 17 kN m^{-1}) [29]. The high tensile strength of the BC network, which formed in between the sisal fibres, provided the mechanical performance of the manufactured BC-sisal fibre preforms (Table 1). The use of BC as binder also reduced the porosity of the fibre preforms as the hornified BC network held the fibres more tightly together. The absolute density of BC-sisal preform is higher than that of neat sisal preform (Table 1). This is due to the incorporation of 10 wt.% BC nanofibres, which are denser, into the BC-sisal preforms. The absolute density of BC was measured to be 1.525 g cm^{-3}.

Table 2
Mechanical properties of neat polyAESO and its composites. v_f, ρ_c, E_T, σ_T, E_F, σ_F, denote the total fibre volume fractions, density of the composites, tensile modulus, tensile strength, flexural modulus and flexural strength, respectively.

Sample	v_f (vol.%)	ρ_c (g cm^{-3})	E_T (GPa)	σ_T (MPa)	E_F (GPa)	σ_F (MPa)
Neat polyAESO	0	1.09 ± 0.01	0.4 ± 0.1	4.1 ± 0.1	0.2 ± 0.1	9.0 ± 0.1
Sisal-polyAESO	40 ± 2	1.17 ± 0.01	3.2 ± 0.2	18.4 ± 0.9	1.9 ± 0.2	28.9 ± 1.6
BC-Sisal-polyAESO	41 ± 3[a]	1.19 ± 0.01	5.6 ± 0.4	31.4 ± 0.5	4.6 ± 0.3	62.4 ± 3.0

[a] v_f of sisal and BC were estimated to be 37 vol.% and 4 vol.%, respectively.

4.2. Mechanical properties of the composites

Both the tensile and flexural properties of neat polyAESO and its composites are summarised in Table 2. The fibre volume fractions of sisal-polyAESO and BC-sisal-polyAESO were found to be 40 vol.%, implying that direct comparisons between sisal-polyAESO and BC-sisal-polyAESO can be made. The porosity of the composites was found to be approximately 3%. This porosity could arise from the fact that lumen of the fibres has not been fully filled by the resin. When sisal fibres were used as reinforcement for polyAESO, the tensile modulus improved from 0.4 GPa for neat polyAESO to 3.2 GPa for 40 vol.% sisal fibre reinforced polyAESO composites. A further improvement of the tensile modulus of the composites from 3.2 GPa to 5.6 GPa was achieved when BC was used as the binder for the natural fibre preform. This is thought to be due to the stiffening of polymer matrix when the fibre preform contained a hornified network of BC. It has been shown that the stiffness of a polymer matrix can be improved by as much as 40% when BC, which has an estimated Young's modulus of 114 GPa [11], at a loading fraction of only 5 wt.% was used [30].

A similar trend was observed for the tensile strength of the composites. Neat polyAESO had a tensile strength of only 4.1 MPa. When neat polyAESO was reinforced with 40 vol.% sisal fibres the tensile strength increased to 18.4 MPa. A further improvement was achieved when 40 vol.% of BC and sisal fibres in form of a preform, were used as reinforcement. The tensile strength of BC-sisal-polyAESO increased by 71% and nearly 700% when compared to sisal-polyAESO and neat polyAESO, respectively. This significant improvement when BC-sisal fibre preforms were used to create composites can be attributed to (i) the enhanced fibre–matrix interaction (see DMTA section) and (ii) enhanced fibre–fibre stress transfer. The use of BC as binder for the fibres resulted in the formation of continuous but hornified BC network, encasing sisal fibres bonding them together. It is postulated that this enhances the fibre–fibre stress transfer compared

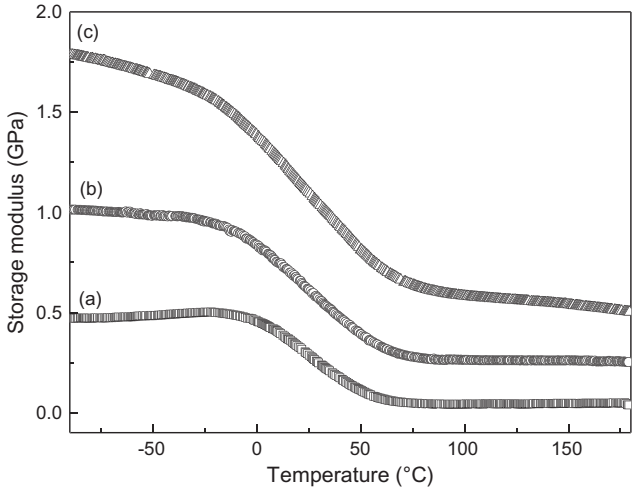

Fig. 3. Visco-elastic behaviour of the composites as a function of temperature. (a) Neat polyAESO, (b) Sisal-polyAESO and (c) BC-Sisal-polyAESO.

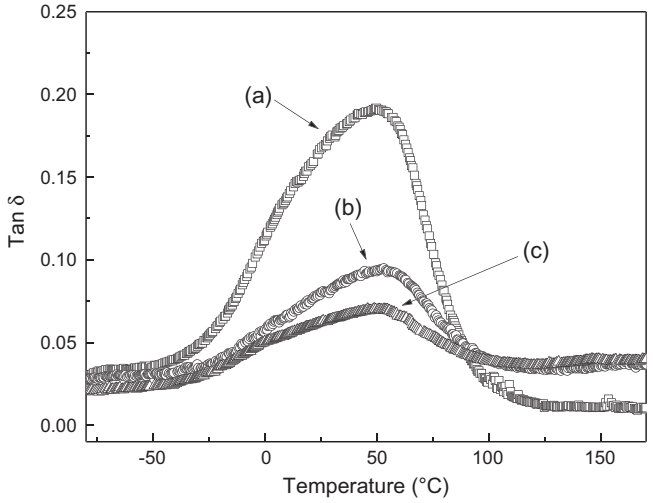

Fig. 4. Tan δ as a function of temperature. (a) Neat polyAESO, (b) Sisal-polyAESO and (c) BC-Sisal-polyAESO.

Table 3
Visco-elastic properties of polyAESO and its composites. G' and G' denote the storage modulus and improvements in storage modulus over neat polyAESO, respectively.

Sample	G' at −95 °C (GPa)	G' at −95 °C (%)	G' at 100 °C (MPa)	G' at 100 °C (%)
Neat polyAESO	0.52 ± 0.01	–	43.4 ± 0.3	–
Sisal-polyAESO	1.02 ± 0.01	96 ± 1	263.3 ± 0.1	501 ± 3
BC-Sisal-polyAESO	1.79 ± 0.01	244 ± 6	580.4 ± 0.6	1237 ± 9

Table 4
The mechanical glass transition temperature (T_g), taken as the peak of tan δ and the quality of fibre–matrix interface (b) of the composites.

Sample	T_g (°C)	b
Neat polyAESO	49 ± 2	–
Sisal-polyAESO	50 ± 3	1.26 ± 0.06
BC-Sisal-polyAESO	50 ± 2	1.54 ± 0.11

to sisal fibre only preforms, where the fibres are mostly isolated. In addition to this, it has been shown that using BC as binder enhances the tensile properties (and, therefore, the handleablity and robustness) of the BC-sisal fibre preforms compared to sisal fibre preforms. This translates to the improved tensile strength of the manufactured BC-sisal-polyAESO.

The flexural modulus and strength of the composites also increased when compared to neat polyAESO (see Table 2). When BC-sisal fibre preforms were used as reinforcement to create composites, improvements over sisal-polyAESO of 142% and 116% were observed in flexural modulus and strength, respectively. As aforementioned, the improvements in the flexural moduli of BC-sisal-polyAESO can be attributed to the inclusion of nano-sized BC, which is an effective stiffening agent, into the polymer matrix. This can be attributed to (i) enhanced mechanical performance of the BC-sisal preforms (see Table 1), (ii) rigid structure of BC and (iii) formation of a 3-dimensional network of rigid nanocellulose within the matrix [30].

4.3. Thermo-mechanical behaviour of the composites

The viscoelastic properties of neat polyAESO and its composites as a function of temperature are shown in Fig. 3. The storage moduli of the composites are markedly higher than that of neat polyAESO. These results corroborate the tensile and flexural properties. The storage moduli stayed relatively constant in the glassy region until T_g, when they sharply decreased. As the temperature is increased further, the storage moduli decreased to a constant value independent of temperature as expected for a thermoset. The increment in the storage moduli at −95 °C of the composites is summarised in Table 3. When sisal preforms were used as reinforcement, only a 96% increase in the storage modulus was observed. When BC-sisal preforms were used instead, a remarkable 244% increase in the storage modulus was observed when compared to neat polyAESO. Improvements in the storage moduli of the composites at 100 °C were also observed (see Table 3).

Tan $\delta = f(T)$ of neat polyAESO and the composites are shown in Fig. 4. Tan δ is a measure of the damping properties of a material. It is also determined by the quality of the fibre–matrix interface in composites expressed as the fibre–matrix interfacial strength indicator b as described by the relationship [31]:

$$b = \frac{\left(1 - \frac{\tan\delta_c}{\tan\delta_m}\right)}{v_f} \tag{3}$$

where tan δ_c, tan δ_m and v_f represent the tan δ of the composite and neat polymer, fibre volume fraction, respectively.

This equation implies that a large tan δ amplitude indicates a weak fibre–matrix interface whereas a small tan δ amplitude indicates a stronger interface. It can be seen from Fig. 4 that BC-sisal-polyAESO had the lowest amplitude of tan δ, which indicates that the sisal fibre-polyAESO interface was enhanced when BC was used as binder for the sisal fibres. The fibre–matrix interfacial strength indicator b is tabulated in Table 4. A larger b value was also observed for BC-sisal-polyAESO compared to sisal-polyAESO. This can be explained by coating the sisal surface with BC in the preforms. It has been shown that coating the surface of sisal fibres with a layer of BC does enhance the fibre–matrix interface in polylactide and cellulose acetate butyrate composites [6,32]. The surface energy of sisal fibres did increase when BC was used, as BC possesses high surface energy [8,32] due to its highly crystalline nature [33]. A higher surface energy should result in better wetting by AESO. These two effects enhanced the fibre–matrix interaction in the composites compared to sisal-polyAESO. These results also corroborate with the mechanical properties of the composites;

BC-sisal-polyAESO had better tensile and flexural properties compared to sisal-polyAESO.

4.4. Thermal degradation behaviour of the composites

The thermal degradation behaviour of neat polyAESO and its composites in N_2 atmosphere is shown in Fig. 5, along with neat sisal and neat BC. Single step degradation can be observed for neat BC in nitrogen atmosphere. This degradation is associated with the cleavage of glycosidic linkage of BC [34]. A two-step degradation behaviour can be seen for neat sisal fibres. The first degradation occurred between 280 and 350 °C, which corresponds to the degradation of non-cellulosic compounds such as hemicellulose and lignin, followed by a second degradation (350–400 °C) that corresponds to the degradation of cellulose [35]. From this figure, it can also be seen that neat polyAESO showed single step thermal degradation behaviour. Two-step degradation behaviour was observed for the composites. The single step degradation of neat polyAESO is due to the random polymer chain scission occurring around 350–400 °C [36]. On the other hand, the observed lower onset degradation temperature of the composites is due to the presence of sisal fibres in the composites. The first step of degradation in the composites is a result of degradation of the fibres occurring around 250 °C [34], followed by a second step of degradation, which is the random chain scission of polyAESO around 350 °C [36] and thermal degradation of crystalline BC. The residual weight of the composites is approximately 10 wt.%. This can be explained by the carbonisation of the natural fibres and BC.

4.5. Micromechanical modelling of the composite stiffness

The Young's moduli of short fibre reinforced composites can be modelled using Cox–Krenchel theory [37,38]. The Cox–Krenchel model can be written as:

$$E_{composite} = \eta_0 \eta_L v_f E_f + (1 - v_f) E_m \tag{4}$$

where $E_{composite}$, η_0, v_f, E_f and E_m represent the calculated Young's modulus of the composites, fibre orientation factor, fibre volume fraction, stiffness of the fibre and matrix, respectively. The limited stress transfer efficiency due to fibres of finite length, η_L, can be obtained from 'shear-lag' model [37]:

$$\eta_L = 1 - \frac{tanh\left(\frac{\beta L}{2}\right)}{\frac{\beta L}{2}} \tag{5}$$

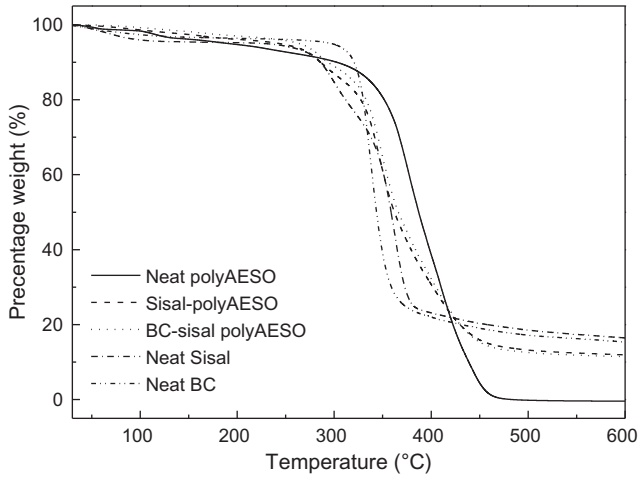

Fig. 5. TGA of sisal fibres, BC, neat polyAESO and its composites.

$$\beta = \frac{2}{d}\left[\frac{2 \times G_m}{E_f ln\left(\sqrt{\frac{\pi}{X_i \times v_f}}\right)}\right]^{0.5} \tag{6}$$

$$G_m = \frac{E_m}{2 \times (1 + v)} \tag{7}$$

where L, d, G_m, X_i and v denote the fibre length, fibre diameter, shear modulus, packing of fibres in the composites and Poisson ratio of the matrix, respectively. Using input parameters of E_f = 24.1 GPa, E_m = 0.4 GPa, η_0 = 0.375, L = 10 mm, d = 0.10 mm, v = 0.34 and X_i = 4.0 (assuming square packing of fibres [39]), a composite stiffness was estimated to be 3.75 GPa for sisal-polyAESO. The slight discrepancy could be due to (i) imperfect fibre–matrix interface and (ii) fibres not possing, a circular cross-section. The Cox–Krenchel model could also be modified to incorporate BC in the equation:

$$E_{composite} = \eta_0 \sum_{i=1}^{n} \eta_{L,i} v_{f,i} E_{f,i} + \left(1 - \sum_{i=1}^{n} v_{f,i}\right) E_m \tag{8}$$

where $\eta_{L,i}$, $v_{f,i}$ and $E_{f,i}$ denote the length efficiency, volume fraction and stiffness of component 'i' in the composites, respectively. This equation assumes that there is no mutual interaction between the reinforcing components. Using the same input parameters for sisal fibres as previously described and assuming a BC modulus of 114 GPa, BC length and diameter of 0.001 mm and 0.00005 mm, respectively, a composite modulus of 3.68 GPa was obtained for BC-sisal-polyAESO. However, this stiffness does not agree with our experimentally measured stiffness for BC-sisal-polyAESO of 5.6 GPa. The mutual interactions between sisal fibres and BC could increase the stiffness of the resulting composites beyond the prediction from 'rule-of-mixture'. However, if one were to assume that BC exists as a continuous (percolating) network in the composites, the Cox–Krenchel model can be re-written as:

$$E_{composite} = \eta_0 (\eta_{L,sisal} v_{f,sisal} E_{f,sisal} + v_{f,BC} E_{f,BC}) + (1 - v_{f,sisal} - v_{f,BC}) E_m \tag{9}$$

where $\eta_{L,sisal}$, $v_{f,sisal}$, $v_{f,BC}$, $E_{f,sisal}$ and $E_{f,BC}$ denote the length efficiency of sisal fibres, volume fractions of sisal fibres and BC in the composites, stiffness of sisal fibres and BC, respectively. It should be noted that the length efficiency of BC was assumed to be unity due to the formation of a continuous (percolating) network in the composites. Using this model, the stiffness of the composites was estimated to be about 5 GPa, which agrees with our experimental value. The slight discrepancy could be due to the fact that interaction between sisal fibres and BC was omitted from the model. Nonetheless, the assumption of the existence of a continuous (percolating) BC network in the composites seems fit our experimental value. The percolating threshold of nanocellulose was estimated to be between 1 and 6 vol.% relative to the polymer matrix, depending on the type of nanocellulose [40] and the BC volume fraction in our composites relative to the matrix was estimated to be 6 vol.%. This suggests our initial assumption of the existence of a continuous (percolating) network within BC-sisal-polyAESO is valid and increases the stiffness of the composites.

4.6. Micromechanical modelling of the composite strength

The strength of a composite material can be predicted using the Kelly–Tyson model with short and aligned fibres [41]. The model can be written as:

$$\sigma_{composite} = \left[\sum_i \frac{L_i v_i}{2L_c} + v_j \sum_j \left(1 - \frac{L_c}{2L_j}\right)\right] \sigma_f + (1 - v_f) \sigma_m \tag{10}$$

where $\sigma_{composite}$, σ_f, σ_m and v_f denote the predicted strength of the composites, fibre strength, matrix strength and fibre volume fraction, respectively. In this equation, Lc represents the critical length of the fibre. v_i is the fibre volume fraction of fibres of length L_i, which is shorter than the critical fibre length and v_j is the fibre volume fraction of fibres with length L_j, which is longer than the critical fibre length. As aforementioned, this equation is valid for discontinuous unidirectional fibres and unlike in the case of stiffness modelling, there is no simple numerical orientation factor to account for the random orientation of the fibres in the composites. However, it is possible to fit the tensile strength data to obtain a 'virtual orientation factor' ($\eta_{0,v}$) account for the random orientation of fibres. Thus, Eq. (10) can be re-written as:

$$\sigma_{composite} = \eta_{0,v}\left[\sum_i \frac{L_i v_i}{2L_c} + v_j \sum_j \left(1 - \frac{L_c}{2L_j}\right)\right]\sigma_f + (1 - v_f)\sigma_m \qquad (11)$$

Thomason et al. [42] found a value of 0.2 for $\eta_{0,v}$ by fitting the experimentally measured tensile strength for randomly oriented discontinuous glass fibre reinforced polypropylene composites. By using input parameters of $\sigma_f = 535$ MPa, $\sigma_m = 4.1$ MPa, $L_c = 6$ mm [43] and $L = 10$ mm, a $\sigma_{composite} = 32.4$ MPa was estimated. This predicted strength value does not reach our experimentally measured value, largely due to the anisotropic nature of sisal fibres compared to glass fibres [44]. Similar results were also observed by van den Oever et al. [45]. The best fit of our experimentally measured value of 18 MPa yielded $\eta_{0,v} = 0.11$. To further predict the tensile strength of BC-sisal-polyAESO, the Kelly–Tyson model can be modified (ignoring mutual interaction between BC and sisal fibres) to incorporate the contribution of BC to the overall strength of the composites:

$$\sigma_{composite} = \eta_{0,v,sisal}\left[\sum_i \frac{L_i v_i}{2L_c} + v_j \sum_j \left(1 - \frac{L_c}{2L_j}\right)\right]\sigma_{f,sisal} + \eta_{0,v,BC}\left[\sum_i \frac{L_i v_i}{2L_c} + v_j \sum_j \left(1 - \frac{L_c}{2L_j}\right)\right]\sigma_{f,BC} + (1 - v_f)\sigma_m \qquad (12)$$

The first and second terms on the right hand side of Eq. (12) represent the contribution of sisal fibres and BC to the overall tensile strength of the composites. Since the critical length of BC is not known and it has been shown that BC exists as a continuous percolating network in the composites, the ratio between L_c and L can be approximated to approach zero. Eq. (12) can be simplified to:

$$\sigma_{composite} = \eta_{0,v,sisal}\left[\sum_i \frac{L_i v_i}{2L_c} + v_j \sum_j \left(1 - \frac{L_c}{2L_j}\right)\right]\sigma_{f,sisal} + \eta_{0,v,BC} v_{f,BC}\sigma_{f,BC} + (1 - v_f)\sigma_m \qquad (13)$$

Using an approximate $\sigma_{f,BC} = 2000$ MPa [46] and $\eta_{0,v,sisal} = 0.11$, the best fit of our experimentally measured value yielded $\eta_{0,v,BC} = 0.2$. Although the tensile strength prediction requires two fitting parameters ($\eta_{0,v,sisal}$ and $\eta_{0,v,BC}$), this analysis shows that both sisal fibres and BC contribute only a small fraction to the overall tensile strength of the composites due to the off-axis orientation of the fibres. Nonetheless, the contribution of BC to the tensile strength of the composites is higher than that of sisal fibres ($\eta_{0,v,sisal} < \eta_{0,v,BC}$). This could be due to the higher surface energy of BC ($\sim$61 mJ m^{-2}, as measured by inverse gas chromatography) [8], which leads to better wetting by the matrix.

5. Conclusions

A novel robust short sisal fibre preform was manufactured using BC as binder, moving away from commonly used polymer binders. The BC-sisal fibre preforms possessed a tensile strength of 13.1 kN m^{-1}, whereas the sisal fibre preforms possess no measureable tensile strength. This implies that BC enhanced the mechanical properties and the fibre–fibre stress transfer of the natural fibre preforms. PolyAESO reinforced with sisal fibre and BC-sisal fibre preforms was manufactured using VARI. The use of BC-sisal preforms improved both the tensile and flexural properties of BC-sisal-polyAESO when compared to sisal-polyAESO and neat polyAESO. The tensile modulus and strength of BC-sisal-polyAESO improved by 75% and 71%, respectively over sisal-polyAESO and 1300% and 600%, respectively over neat polyAESO. A similar trend was also observed for the flexural properties of the composites. The flexural modulus and strength of BC-sisal-polyAESO improved by 142% and 116%, respectively over sisal-polyAESO and 2200% and 590%, respectively over neat polyAESO. DMTA confirmed the increase in storage moduli of BC-sisal-polyAESO compared to neat polyAESO and sisal-polyAESO. A decrease in the amplitude of tan δ of BC-sisal-polyAESO compared to sisal-polyAESO was also observed, indicating an enhanced fibre–matrix interface when BC was used as binder. The mechanical properties of the composites were also fitted with micromechanical models. These new types of natural fibre preform reinforced composites offer promising alternative bio-based materials for the industry.

Acknowledgements

The authors greatly appreciate the funding provided by the UK Engineering and Physical Science Research Council (EPSRC) for KYL (EP/F032005/1) and an Imperial College London Deputy Rector's Award for funding the tuition fees of KYL.

References

[1] Thomas S, Paul SA, Pothan LA, Deepa B. Natural fibres: structure, properties and applications. In: Kalia S, Kaith BS, Kaur I, editors. Cellulose fibers: bio- and nano-polymer composites. Berlin: Springer-Verlag; 2011. p. 3–42.
[2] Karnani R, Krishnan M, Narayan R. Biofiber-reinforced polypropylene composites. Polym Eng Sci 1997;37(2):476–83.
[3] Mohanty AK, Misra M, Hinrichsen G. Biofibres, biodegradable polymers and biocomposites: an overview. Macromol Mater Eng 2000;276(3–4):1–24.
[4] Bismarck A, Mishra S, Lampke T. Plant fibers as reinforcement for green composites. In: Mohanty AK, Misra M, Drzal L, editors. Natural fibers, biopolymers and biocomposites. Boca Raton: CRC Press; 2005.
[5] Kalia S, Kaith BS, Kaur I. Pretreatments of natural fibers and their application as reinforcing material in polymer composites-a review. Polym Eng Sci 2009;49(7):1253–72.
[6] Juntaro J, Pommet M, Kalinka G, Mantalaris A, Shaffer MSP, Bismarck A. Creating hierarchical structures in renewable composites by attaching bacterial cellulose onto sisal fibers. Adv Mater 2008;20(16):3122–6.
[7] Juntaro J, Pommet M, Mantalaris A, Shaffer M, Bismarck A. Nanocellulose enhanced interfaces in truly green unidirectional fibre reinforced composites. Compos Interfaces 2007;14(7–9):753–62.
[8] Pommet M, Juntaro J, Heng JYY, Mantalaris A, Lee AF, Wilson K, et al. Surface modification of natural fibers using bacteria: depositing bacterial cellulose onto natural fibers to create hierarchical fiber reinforced nanocomposites. Biomacromolecules 2008;9(6):1643–51.
[9] Iguchi M, Yamanaka S, Budhiono A. Bacterial cellulose – a masterpiece of nature's arts. J Mater Sci 2000;35(2):261–70.
[10] Czaja W, Romanovicz D, Brown RM. Structural investigations of microbial cellulose produced in stationary and agitated culture. Cellulose 2004;11(3–4):403–11.
[11] Hsieh YC, Yano H, Nogi M, Eichhorn SJ. An estimation of the Young's modulus of bacterial cellulose filaments. Cellulose 2008;15(4):507–13.
[12] Eichhorn SJ, Dufresne A, Aranguren M, Marcovich NE, Capadona JR, Rowan SJ, et al. Review: current international research into cellulose nanofibres and nanocomposites. J Mater Sci 2010;45(1):1–33.
[13] Nishino T, Matsuda I, Hirao K. All-cellulose composite. Macromolecules 2004;37(20):7683–7.
[14] Lee K-Y, Bharadia P, Blaker JJ, Bismarck A. Creating hierarchical structures in short sisal fibre reinforced poylactide; short hairy fibre reinforced bacterial cellulose nanocomposites, submitted for publication. http://dx.doi.org/10.1016/j.compositesa.2012.06.013.
[15] Salim MS, Ishak ZAM, Hamid SA. Effect of stitching density of nonwoven fiber mat towards mechanical properties of kenaf reinforced epoxy composites produced by resin transfer moulding (RTM). In: Sapuan SM, Mustapha F, Majid

DL, Leman Z, Ariff AHM, Ariffin MKA, et al., editors. Composite Science and Technology, Pts 1 and 2, vol. 471-4722011. p. 987–92.
[16] Xue DS, Miao MH, Hu H. Permeability anisotropy of flax nonwoven mats in vacuum-assisted resin transfer molding. J Text Inst 2011;102(7):612–20.
[17] Rong MZ, Zhang MQ, Liu Y, Zhang ZW, Yang GC, Zeng HM. Effect of stitching on in-plane and interlaminar properties of sisal/epoxy laminates. J Compos Mater 2002;36(12):1505–26.
[18] Tao WY, Calamari TA, Crook L. Carding kenaf for nonwovens. Text Res J 1998;68(6):402–6.
[19] Du YC, Zhang JL, Toghiani H, Lacy TE, Xue YB, Horstemeyer MF, et al. Kenaf bast fiber bundle-reinforced unsaturated polyester composites. I: processing techniques for high kenaf fiber loading. For Prod J 2010;60(3):289–95.
[20] Ramaswamy GN, Sellers T, Tao WY, Crook LG. Kenaf nonwovens as substrates for laminations. Ind Crops Prod 2003;17(1):1–8.
[21] Åkesson D, Skrifvars M, Walkenström P. Preparation of thermoset composites from natural fibres and acrylate modified soybean oil resins. J Appl Polym Sci 2009;114(4):2502–8.
[22] O'Donnell A, Dweib MA, Wool RP. Natural fiber composites with plant oil-based resin. Compos Sci Technol 2004;64(9):1135–45.
[23] Garkhail SK, Heijenrath RWH, Peijs T. Mechanical properties of natural-fibre-mat-reinforced thermoplastics based on flax fibres and polypropylene. Appl Compos Mater 2000;7(5–6):351–72.
[24] Heijenrath R, Peijs T. Natural-fibre-mat-reinforced thermoplastic composites based on flax fibres and polypropylene. Adv Compos Lett 1996; 5(3):81–5.
[25] Reck B, Turk J. Thermally curable aqueous acrylic resins – a new class of duroplastic binders for wood and natural fibers. Angew Makromol Chem 1999;272:5–10.
[26] Blaker JJ, Lee KY, Bismarck A. Hierarchical composites made entirely from renewable resources. J Biobased Mater Bioenergy 2011;5(1):1–16.
[27] Schlufter K, Schmauder HP, Dorn S, Heinze T. Efficient homogeneous chemical modification of bacterial cellulose in the ionic liquid 1-N-butyl-3-methylimidazolium chloride. Macromol Rapid Commun 2006; 27(19):1670–6.
[28] Diniz J, Gil MH, Castro J. Hornification – its origin and interpretation in wood pulps. Wood Sci Technol 2004;37(6):489–94.
[29] Zhou Q, Malm E, Nilsson H, Larsson PT, Iversen T, Berglund LA, et al. Nanostructured biocomposites based on bacterial cellulosic nanofibers compartmentalized by a soft hydroxyethylcellulose matrix coating. Soft Matter 2009;5(21):4124–30.
[30] Lee KY, Blaker JJ, Bismarck A. Surface functionalisation of bacterial cellulose as the route to produce green polylactide nanocomposites with improved properties. Compos Sci Technol 2009;69(15–16):2724–33.
[31] Afaghi-Khatibi A, Mai YW. Characterisation of fibre/matrix interfacial degradation under cyclic fatigue loading using dynamic mechanical analysis. Composites A 2002;33(11):1585–92.
[32] Heng JYY, Pearse DF, Thielmann F, Lampke T, Bismarck A. Methods to determine surface energies of natural fibres: a review. Compos Interfaces 2007;14(7–9):581–604.
[33] Papirer E, Brendle E, Balard H, Vergelati C. Inverse gas chromatography investigation of the surface properties of cellulose. J Adhes Sci Technol 2000;14(3):321–37.
[34] U.S.D.A. Thermal degradation of wood components, Madison: U.S. Department of Agriculture, Forest Service, Forest Laboratory; 1970.
[35] Martin AR, Martins MA, da Silva O, Mattoso LHC. Studies on the thermal properties of sisal fiber and its constituents. Thermochim Acta 2010;506(1–2): 14–9.
[36] Behera D, Banthia AK. Synthesis, characterization, and kinetics study of thermal decomposition of epoxidized soybean oil acrylate. J Appl Polym Sci 2008;109(4):2583–90.
[37] Cox HL. The elasticity and strength of paper and other fibrous materials. Br J Appl Phys 1952;3:72–9.
[38] Krenchel H. Fibre-reinforcement – theoretical and practical investigation of the elasticity and strength of fibre-reinforced materials. Technical University of Denmarck; 1964.
[39] Thomason JL, Vlug MA. Influence of fibre length and concentration on the properties of glass fibre-reinforced polypropylene: 1. Tensile and flexural modulus. Compos Part a – Appl Sci Manuf 1996;27(6):477–84.
[40] Siqueira G, Bras J, Dufresne A. Cellulosic bionanocomposites: a review of preparation. Prop Appl Polym 2010;2(4):728–65.
[41] Kelly A, Tyson WR. Tensile properties of fibre-reinforced metals. J Mech Phys Solids 1965;13(6):329–38.
[42] Thomason JL, Vlug MA, Schipper G, Krikor H. Influence of fibre length and concentration on the properties of glass fibre-reinforced polypropylene: 3. Strength and strain at failure. Compos Part a – Appl Sci Manuf 1996;27(11): 1075–84.
[43] Li Y, Mai YW, Ye L. Sisal fibre and its composites: a review of recent developments. Compos Sci Technol 2000;60(11):2037–55.
[44] Thomason JL. Dependence of interfacial strength on the anisotropic fiber properties of jute reinforced composites. Polym Compos 2010;31(9):1525–34.
[45] van den Oever MJA, Bos HL, van Kemenade M. Influence of the physical structure of flax fibres on the mechanical properties of flax fibre reinforced polypropylene composites. Appl Compos Mater 2000;7(5–6):387–402.
[46] Yano H, Sugiyama J, Nakagaito AN, Nogi M, Matsuura T, Hikita M, et al. Optically transparent composites reinforced with networks of bacterial nanofibers. Adv Mater 2005;17(2):153–+.